Simulation Based Ankle Injury Evaluation using GHBMC Modular Human Body Models.

Tejas Ruparel, Vikas Hasija, Erik Takhounts

Abstract Lower extremity injuries, especially in the foot and ankle region, are frequent and severe in frontal automotive collisions and often lead to impairment and long-term disabilities. Such injuries are also more common among female drivers, than male, in comparable motor vehicle crashes. Since these injuries can lead to costly rehabilitation, it is important to better understand their distribution and causation among different sexes. Accordingly, the goal in this study is to utilise biofidelic human body models to simulate foot and ankle injuries when the occupant is subject to a wide range of field representative frontal impact scenarios, and to investigate the distribution of ankle injuries among females and males. We also investigated the effects of different foot placements, brake pedal vs toepan, on resulting injuries. To achieve this, we employed the Design of Experiments approach to simulate over 300 frontal impact scenarios with variations in vehicle crash parameters and relative occupant positions. We also introduced a new bone fracture criteria to reliably identify skeletal injuries. Simulated results show that females have a greater risk of ankle injury than males, and the right foot (positioned on the brake pedal) has higher risk of ankle injuries than the left foot (positioned in the toepan).

Keywords Ankle injuries, bone fracture criteria, design of experiments, frontal crashes, human body models.

I. INTRODUCTION

Automotive safety has significantly improved over the past few decades and resulting trends have shown a significant drop in total number of crash induced injuries since the late 1990s [1]. The introduction of new and improved Federal Motor Vehicle Safety Standards (FMVSS) has also led to a decline in the total number of injuries [2]. Since advancements in safety systems such as airbags [3] and seatbelts with pretensioners and load-limiters [4-5] have helped improve protection in the head, neck, and the torso body region, Lower Extremity Injuries (LEIs) are now the most frequent site for Abbreviated Injury Scale (AIS)2+ injuries. In a recent study, [6] analysed National Highway Traffic Safety Administration's (NHTSA) 1998–2015 National Automotive Sampling System Crashworthiness Data System (NASS-CDS) data (weighted) for belted occupants involved in a crash with a Principal Direction of Force (PDOF) between ±60° (near/far side) and showed that the lower extremity body region sustained the highest number of AIS2+ injuries (Fig. 1 (a)). They further analysed the weighted dataset for 2009+ model year vehicles and found that highest number of LEIs occurred in the foot and ankle region (Fig. 1 (b)).

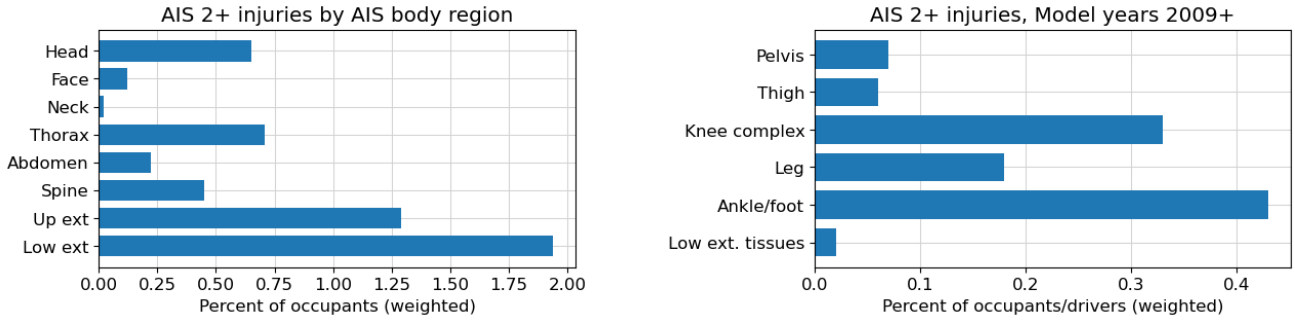

(a) (b)

Fig. 1. AIS2+ injuries (a) within each AIS body region and (b) within lower extremities. Reproduced from [6]

Although LEIs are rarely life-threatening, they can often lead to long-lasting disabilities with physical and psychosocial effects [7]. Due to the frequency and severity of these injuries, many studies have investigated identifying, quantifying, and predicting the risk of foot and ankle injuries. Such investigations are typically conducted on human surrogates such as post-mortem human subjects (PMHSs), Anthropomorphic Test Devices

Tejas Ruparel is a Crash Simulation Engineer at Bowhead Mission Solutions (tejas.ruparel.ctr@dot.gov, +1 202-355-8571). Vikas Hasija and Erik Takhounts are both Mechanical Engineers with the Human Injury Research Division at the Department of Transportation National Highway Traffic Safety Administration, USA.

(ATDs), or by utilising real-world/field data from NASS-CDS or Crash Injury Research and Engineering Network (CIREN) databases. Several other studies have investigated and compared injury risks between females and males in comparable motor vehicle crashes (MVCs), highlighting that females are more susceptible to crash induced injuries than males, with significantly higher occurrence of LEIs [8-11]. In their investigation, reference [6] concluded that females are at a greater risk of AIS2+ and AIS3+ injuries compared to males, with the odds ratio of 3.05 for LEIs and 3.8 for foot and ankle injuries.

Despite the extensive knowledge base accumulated from human surrogate testing and real-world/field data analysis, the key contributing factors related to foot and ankle injury and their mechanisms remain unclear. Accordingly, the goal of this study is to utilise human body Finite Element (FE) models to simulate foot and ankle injuries (ligamentous and skeletal/bone fractures), and to investigate their distribution among females and males under similar real-world crash conditions. To achieve this, we utilised the Global Human Body Model Consortium (GHBMC) FE models, positioned in a simplified vehicle compartment, to simulate a wide range of frontal impact scenarios using the Design of Experiments (DOE) method. The variations in vehicle crash parameters, such as change in velocity (Delta-V) and Principal Direction of Force (PDOF), were sampled to simulate the real-world/field distribution to produce field representative distribution of injuries. We also introduce and compare various bone fracture criteria for reliable classification of skeletal injuries across all analysed Human Body Models (HBMs). And finally, we also investigated the effects of different foot placements, with the right foot positioned on the brake pedal and the left foot positioned in the toepan to gain additional insights into injury mechanisms due to distinct boundary conditions.

II. METHODS

The following section describes our approach in simulating foot and ankle injuries among females and males, starting with the FE vehicle model, utilised FE HBMs, occupant positioning, injury assessment, and the overall scope for the field representative DOE.

Vehicle Model

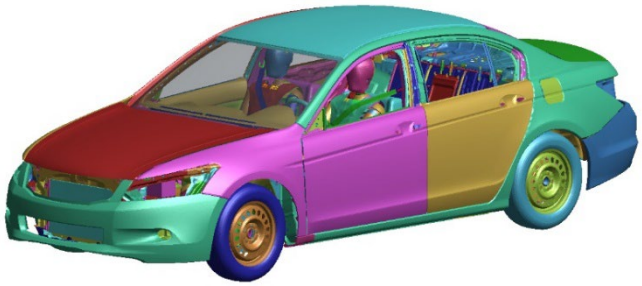

Fig. 2. 2014 Honda Accord FE model.

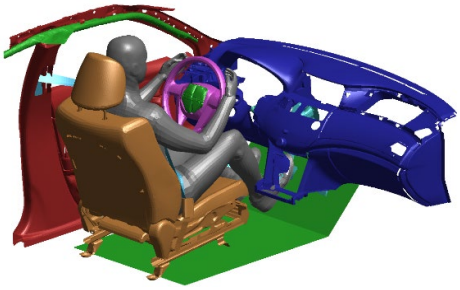

Fig. 3. Simplified occupant compartment model.

A validated 2014 Honda Accord FE model (Fig. 2) [12] was selected for this study. To simulate a wide range of frontal impact scenarios within a feasible timeframe, a simplified occupant compartment model (Fig. 3) was created by extracting the necessary components from the full vehicle model. This simplified model consisted of vehicle floor, bodyside structure including door panel, B-pillar, A-pillar, roof-rail inner, the instrumentation/dash panel including knee bolster and collapsible steering column, deformable driver seat, and safety restraint systems such as frontal/side airbags and seatbelts (including retractor, pretensioner, and load limiter). The simplified occupant compartment model also included the accelerator/brake pedal assembly (Fig. 9 (b)) which allowed for different foot placements, hence distinct boundary conditions for comprehensive injury assessment. The baseline moment rotation curve for the brake pedal (Fig. 4) was obtained from [13], and had a stop angle of 7.4° and an MR-AUC of 22 J. Introducing the brake pedal also allowed us to investigate the effects of stop angle and rotational stiffness, expressed in terms of the area under the moment rotation curve (MR-AUC), on the resulting injuries. Accordingly, brake pedal stop angle and rotational stiffness were parametrised and introduced as DOE design variables. The parameter for brake pedal stop angle (BPSA), scaled the MR curve along its abscissa by the factor BPSA/7.4, and the parameter for brake pedal rotational stiffness (BPRS) scaled the MR curve along its ordinate by the factor BPRS*7.4/BPSA. These scaling factors ensured that the parameters BPSA and BPRS could be updated individually or together.

Since oblique impacts are usually more severe in terms of injury risk than full-frontal impacts at same Delta-V, the baseline crash pulse (Fig. 5) was obtained from NHTSA test 9476 [14] for a 2015 Chevrolet Malibu frontal-oblique impact with 35% overlap. This crash pulse had a peak acceleration of 38 g and a Delta-V of 33 mph. The vehicle crash pulse was also parametrised by scaling the magnitude/acceleration, resulting in Delta-Vs ranging from 5 to 35 mph (TABLE III). Although ankle injuries may also be affected by the shape of the pulse, the profile was not parametrised to keep the design variables, and hence the overall scope of the DOE, to a manageable size.

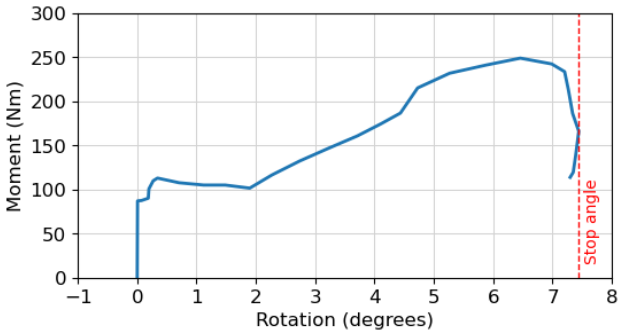

Fig. 4. Brake pedal moment vs rotation curve.

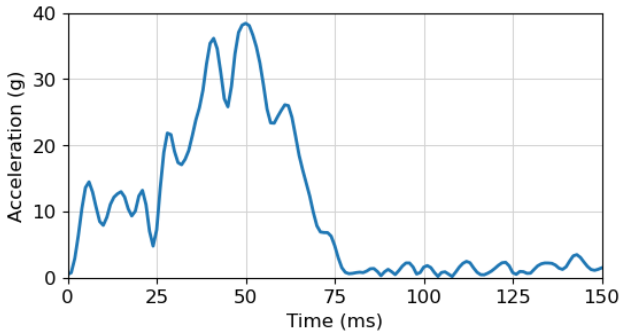

Fig. 5. Vehicle crash pulse.

GHBMC Modular Human Body Models

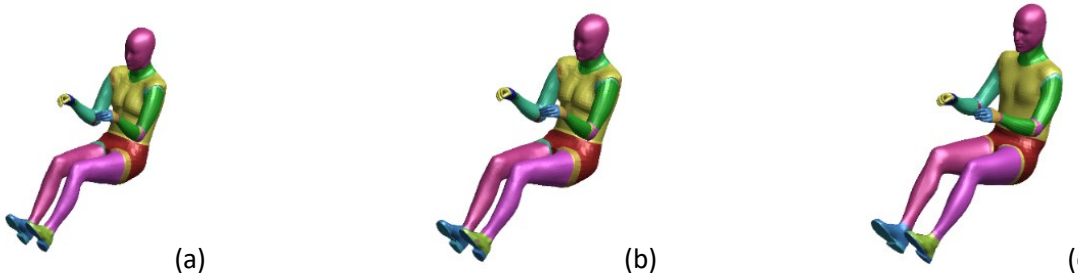

(a) (b) (c)

Fig. 6. GHBMC modular human body models (a) 5th female (b) 50th female (scaled) and (c) 50th male.

The study utilised validated 5th percentile adult female (F05) (Fig. 6 (a)) and 50th percentile adult male (M50) (Fig. 6 (c)) modular lower extremity GHBMC FE models. Modular models (Fig. 7), with their simplified upper body and pelvis and detailed lower extremities, maintain model fidelity in the foot and ankle region while lowering simulation runtimes, which is favourable for the DOE. The lower extremity Body Region Model (BRM) includes 1D/3D representation of muscles, 1D/2D representation of ligaments and tendons, and 2D/3D representation of bones [15-16]. These models also include pre-programmed parameters to assess Crash Induced Injuries (CIIs) such as cortical bone fracture and ligament failure.

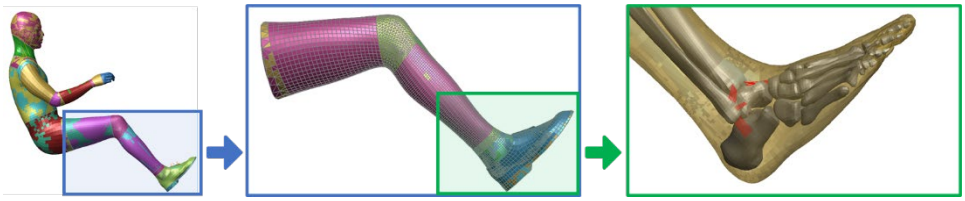

Fig. 7. GHBMC modular HBM with simplified upper body/pelvis, detailed lower extremity BRM and ankle joint.

In addition to the validated F05 and M50 HBMs, a 50th percentile adult female HBM (F50s, s for scaled) (Fig. 6 (b)) was also utilised in this study. This F50s model was generated by uniformly scaling the validated F05 HBM by a factor of 1.1, which is the seated height ratio between F50s and F05 [17]. The mass for this F50s HBM, after uniform scaling, was 67.6 kg and similar to the mass reported by [18] (62.3 kg) for the anthropometric measures of a 50th percentile female. Although this model does not represent the true 50th percentile adult female, it can provide useful insights regarding injury risks based on size and seating position, by representing the anthropometry of a mid-sized female. TABLE I provides an overview of analysed HBMs, their sizes, mass and sitting heights.

TABLE I
GHBMC (MODULAR LOWER EXTREMITY) HBM

Model	Nodes	Elements	Mass (kg)	Seated height (mm)
5th percentile adult female (F05)	568,552	795,863	52.2	776
50th percentile adult female (F50s)	568,552	795,863	67.6	856
50th percentile adult male (M50)	478,852	577,340	76.5	912

Occupant Positioning

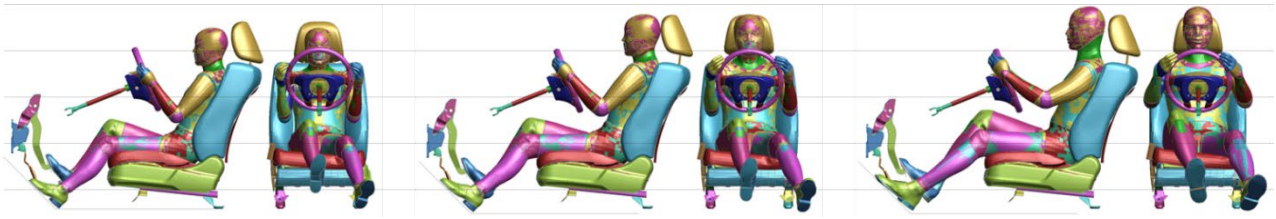

(a) (b) (c)

Fig. 8. Occupant positioning (a) F05 (b) F50s and (c) M50.

F05 and M50 were positioned in the simplified occupant compartment model (Fig. 8) following the dummy positioning procedures for driver test dummy conforming to Subpart E of PART 572 [19]. Reference positional measurements such as the knee to dash (KD), chest to steering (CS) and knee to knee distance (KK), as shown in Fig. 9 (a), for F05 and M50 were obtained from representative NHTSA tests, 8380 and 8035 [19-20], respectively. Occupant specific KK distance from these tests was first used to position the right foot on the accelerator pedal and left foot in the toepan, conforming to the dummy positioning procedures. The right foot was then re-positioned onto the brake pedal (Fig. 9 (b)) to account for pre-impact braking and to introduce distinct boundary conditions, resulting in lower KK than the respective test measurements.

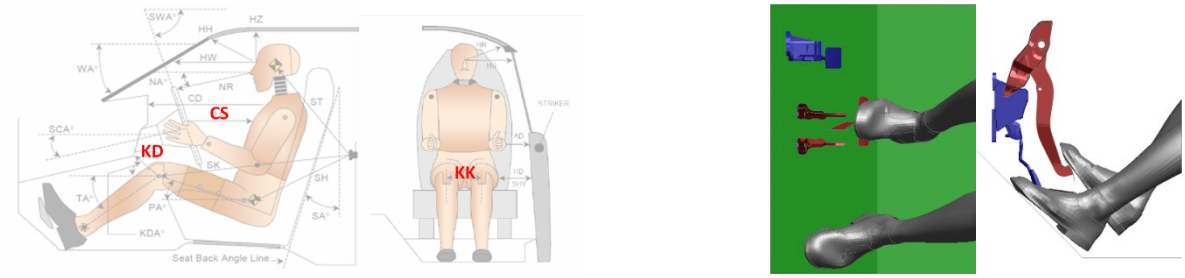

(a) (b)

Fig. 9. Occupant positioning (a) reference measurements (b) right vs left foot positioning.

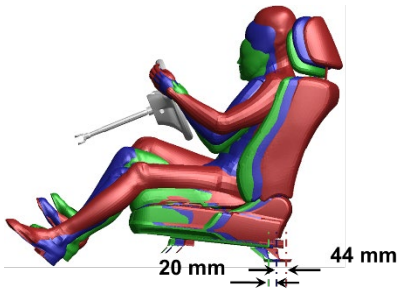

Fig. 10. Final seating position for F05 (green), F50s (blue) and M50 (red) and respective seat track offsets.

Since there is no procedure outlined for positioning F50s, it was first positioned in the same seat track position as the M50. In this position, the feet of F50s were not in contact with the toepan, subsequently the seat was moved forward on the track such that the feet were in contact with the toepan. This procedure resulted in F50s being 20 mm rearward and 44 mm forward in the seat track position than F05 and M50, respectively (Fig. 10). The KK distance for F05 from NHTSA test 8380 was also scaled up by a factor of 1.1 to obtain the reference KK for F50s. After positioning the HBM in the simplified occupant compartment, LS-DYNA pre-simulations were used for seat foam compression, followed by seat belt routing and fitting. The seat compression simulations did not change the relative position of the HBM since they were simulated using a rigid outer shell for the occupant that compressed the seat cushion under loads from the boundary prescribed motion of the HBM.

Injury assessment:

Given the extent of available CIIs in the foot and ankle region of the GHBMC HBMs, we monitored nine ligaments (ATiF, ATaF, CF, PTiF, PTaF, PTT, TiC, ATT, and TiN) and four bones (Calcaneus, Talus, Malleolar Tibia and Malleolar Fibula) for potential injuries across all occupant models (Fig. 11).

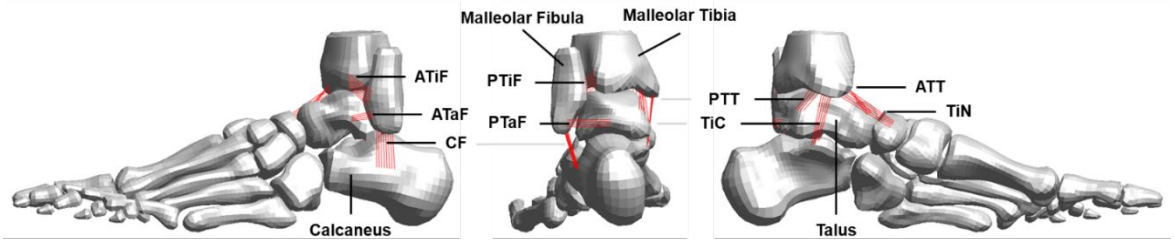

Fig. 11. Analysed ankle injuries, lateral, posterior, and medial views.

Ankle ligaments within these HBMs are modelled as beam elements (nonlinear 1D spring) and their respective failure parameters, modelled as translational displacement at failure under tension (UTFAIL), are based on the maximum force within the ligament when subject to dorsiflexion/plantarflexion, inversion/eversion, and combined loading conditions [16]. Ligament failure in the GHBMC models is programmed with element deletion and hence ligamentous CIIs are assumed to occur at first beam failure/deletion. Since very limited test data exists on the mechanical behaviour of ankle ligaments for males vs females [21-23], the failure strain (based on relaxed ligament lengths and corresponding UTFAIL) was equalised across all three HBMs, with M50 as the reference.

Skeletal injuries or bone fractures were monitored for the cortical layer and modelled based on the Maximum Principal Strain (MPS), 2% for calcaneus/talus and 1.5% for malleolar tibia/fibula [15-16]. The failure parameter in this case is not programmed into the model, i.e., no element deletion, and hence MPS outputs were used for each bone and resulting fractures were identified within the post-processing stage. To ensure reliable predictions across all HBMs, we evaluated skeletal injuries using several different bone fracture criteria by marching in time over the MPS time-history outputs and stopping once the selected criterion had registered a fracture. Refer to Fig. 12 and TABLE II to better understand these criteria and resulting injury predictions.

MPS Using this default injury criterion, fracture is registered if MPS in any element exceeds the set failure strain. This criterion therefore captures the onset of fracture but fails to filter out any spurious strains in elements that might occur due to any numerical instability.

MPS-95 The MPS-x criterion registers fracture only if the x^{th} percentile element exceeds failure strain. Accordingly, only case (e) (Fig. 12 and TABLE II) registers fracture since 5 out of 100 (for x = 95) elements exceed failure strain. This criterion hence ensures that fracture is not registered due to one single element exceeding failure strain. However, it still does not ensure that spurious element strains are filtered out. For example, either of the elements A1, C3 or E5 in Fig. 12 (e) may be considered spurious. MPS-x is also not consistent when applied over different bones or HBMs. For example, the Calcaneus bone has 834 elements in M50, and 510 elements in F05, due to relative size differences. Hence using MPS-95, calcaneus fracture in M50 would depend on 42 elements, whereas in F05 it would depend on 25 elements exceeding the failure strain. In addition, it is not clear whether MPS-95 should be used as a criterion, as opposed to MPS-97 or MPS-93. Hence, this criterion may or may not be related to fractures.

NE-2 The NE-2 criterion registers fracture only when 2 or more Neighbouring Elements (NE-2) exceed failure strain at a given timestep. Hence, any single elements with spurious strains are filtered out. For example, Fig. 12 (c) does not register a fracture since either of C3 or H8 could be spurious, however, Fig. 12 (d) and Fig. 12 (e) do register fracture since a local cluster of 2+ elements (H7, H8 and G8) exceeds failure strain.

NET-2 This criterion extends the capabilities of NE-x by considering the Time (NET-x) difference between the individual elements exceeding the failure strain in the local cluster. For example, Fig. 12 (d) will register fracture only if H7, H8 and G8 have all exceeded failure strain within a predefined time-window. If H7 and G8 exceed failure strain before the set time window, they are considered spurious and ignored, hence no fracture is registered. This allows the user to define a specific time-window, similar to the crack initiation-propagation time delta, to reliably predict bone fractures. In this study, we enforced a time constrain of T = 0.3 ms and hence, a fracture was registered only if the constituent (neighbouring) elements from the NE-2 cluster exceeded the failure strain within 0.3 ms.

Note: Spurious strains, within the scope and context of this investigation, are defined based on single elements that exceed failure strain without any of its neighbours exceeding the same failure criteria. We enforced this definition to systematically filter out cases in which a fracture could be registered either due to local or numerical instabilities.

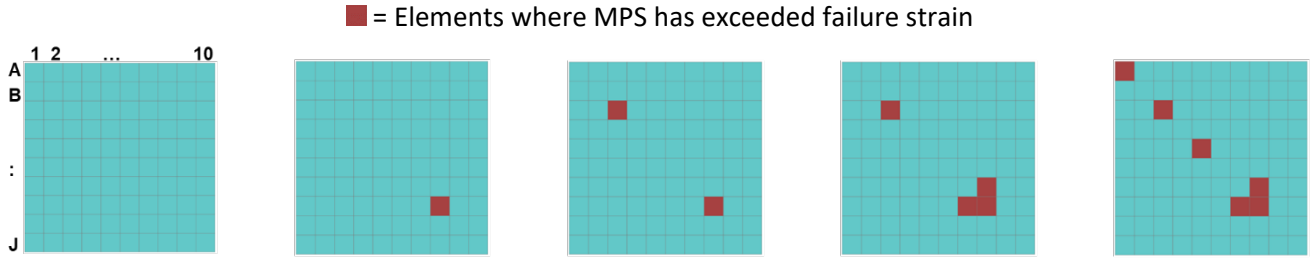

Fig. 12. Schematic for cortical bone fracture criterion.

TABLE II
BONE FRACTURE CRITERION AND RESPECTIVE INJURY PREDICTIONS

Bone fracture criteria	Case (a)	Case (b)	Case (c)	Case (d)	Case (e)
MPS	False	True	True	True	True
MPS-95	False	False	False	False	True
NE-2	False	False	False	True	True
NET-2	False	False	False	True/False	True/False

In addition to using these criteria to identify and register bone fractures within the post-processing stage, we also monitored the maximum MPS in each bone, and the maximum MPS per foot (out of four bones) to obtain a continuous variable for crash sensitivity analysis.

Design of Experiments (DOE)

To investigate the injury risks, paired simulations were run for all three HBMs using the DOE method in LS-OPT [24]. The design variables used to generate a wide range of frontal impact scenarios are provided in TABLE III. A total of 302 points were generated by discretely sampling the seven design variables (six representing the vehicle crash parameters and one representing the relative position of the occupant from the dash panel) for each HBM. Since the right foot was positioned on the brake pedal, and left foot in the toepan, the DOE dataset, stratified by left/right foot, resulted in a total of 604 data points per HBM.

TABLE III
DOE DESIGN VARIABLES ARE THEIR MIN/MAX RANGES

Design Variable	Units	Baseline	Minimum	Maximum
Delta-V	MPH	35	5	35
PDOF	°	0°	-30	+30
Seatbelt load limiter (SLL) force	kN	3	3	5
Seatbelt pretensioner (SP) force	kN	1	1	3
Brake pedal stop angle (BPSA)	°	7.4	3.4	11.4
Brake pedal rotational stiffness (BPRS)	%	100	50	150
Normalised knee to dash distance (NKD)	%	100	75	125
- *F05 knee to dash distance*	Mm	126	94.5	157.5
- *F50s knee to dash distance*	Mm	122	91.5	152.5
- *M50 knee to dash distance*	Mm	168	126	210

The baseline crash pulse (Fig. 5), with a peak acceleration of 38 g and a Delta-V of 33 mph, was scaled in magnitude (ordinate) to provide a wide range of Delta-Vs ranging from 5 to 35 mph. The NASS-CDS data for MVCs between 2010 and 2015 showed that most crashes occur at lower Delta-Vs, in the range of 10 – 15 mph [25]. Delta-V was therefore sampled to appropriately mimic the field distribution, as shown in Fig. 13 (a). Similar NASS-

CDS analysis for frontal crashes (2000 – 2015) within the PDOF range of ±40° showed that the PDOF distribution is very close to normal with the maximum at 0° (full-frontal) representing approximately half of all the crashes [26]. Accordingly, PDOF was also varied between ±30°, as shown in Fig. 13 (b), to replicate the field distribution. The seatbelt load limiter force was varied from 3 – 5 kN, and the pretensioner force from 1 – 3 kN, while ensuring that the pretensioner force was always less than or equal to the load limiter force. The brake pedal stop angle was varied from 3.4° – 11.4°, and its rotational stiffness (expressed in terms of area under the moment rotation curve) was varied by ±50% from its nominal value. The relative position of the occupant, with respect to the vehicle dash panel and the knee bolster, was also varied in this study by moving the knee bolster by ±25% from its nominal position. Although real-life crashes have several other variables, we limit the variables under analysis to those listed in TABLE III to keep the size of the DOE manageable. All design variables, except for Delta-V and PDOF, were sampled using uniform distribution between the lower and upper bounds defined in TABLE III.

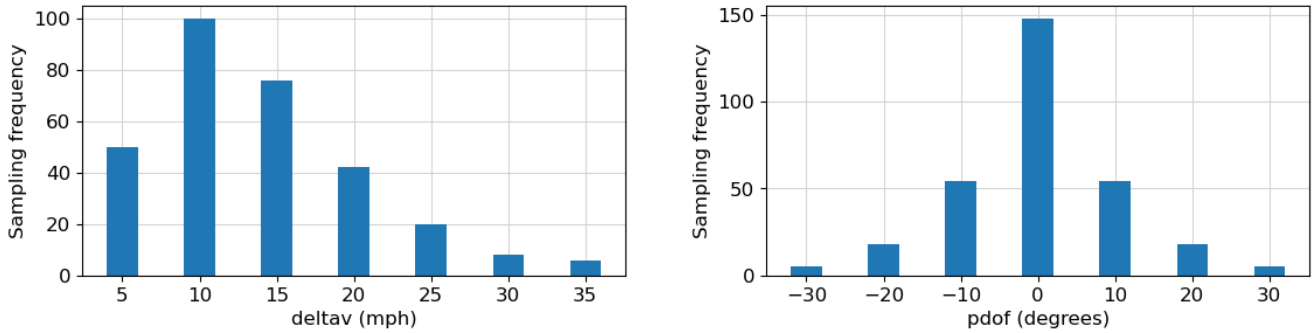

(a) (b)

Fig. 13. DOE sampling for (a) Delta-V and (b) PDOF, representing their respective field distributions.

Note: Normalised knee to dash distance and brake pedal stop angle had a strong correlation post sampling, hence we have excluded brake pedal stop angle as an independent variable from our results and discussion. Also note that no single design variable combinations from TABLE III represents the tested vehicles from test 8380 and 8035 [19-20]. These combinations rather represent a wide range of mid-size sedans, hence representing, to a degree, the field variability in motor vehicles.

III. RESULTS

All three DOEs (F05, F50s and M50) were successfully executed via LS-OPT, and its simulation data and time-histories were post-processed and analysed using an in-house Python code. Figure 14 (a) shows the comparison of AIS2+ ligamentous injuries, stratified by left and right foot, across all three HBMs. Although the HBMs included ligament failure, we did not account for PTT, PTiF and TiN failure as ligamentous injuries due to the lack of sufficient failure test samples available for these ligaments [21]. For the remainder ligaments, injury counts are based on the 1st occurrence of ligament failure, among all 302 exposed cases per foot. We see that both F05 and F50s show relatively higher injuries in the right foot than left foot, and that female HBMs show significantly higher ligamentous injuries than the male HBM, specifically with a combined (left + right) odds ratio of 12.07 for F05 and 5.13 for F50s. The distribution of all ligamentous injuries (not just 1st) by sex is shown in Fig. 14 (b), and it shows that Posterior Talo Fibular ligament (PTaF) has the highest risk of injury for all three HBMs.

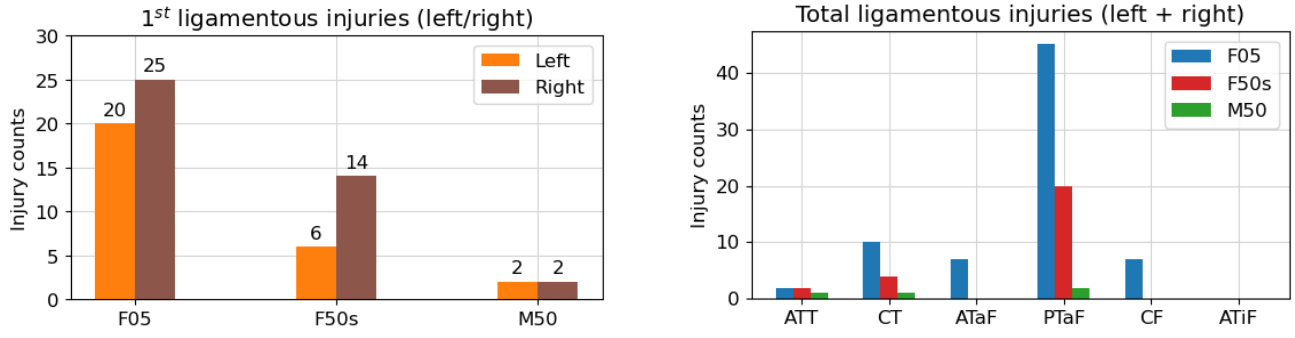

(a) (b)

Fig. 14. (a) AIS2+ ligamentous injuries and (b) distribution of total ligamentous injuries.

Figure 15 (a) shows the comparison of AIS2+ skeletal injuries (or bone fractures) across all HBMs using the bone fracture criteria discussed in Table II. It was observed that MPS showed significantly higher injuries than the other criteria, while MPS-95 filtered out most injuries for M50 (from 104 to 4) and registered zero injuries for F05 and F50s HBMs. NE-2 effectively filters out fractures that might be registered due spurious single element strains by ensuring that only element clusters (of size 2 or more) that exceeded failure strain were registered as fractures. NET-2 further filtered any element clusters in which constituent elements exceeded failure strain with a time lag of over 0.3 ms. Although we chose to present NET-2 results enforced with a 0.3 ms time constraint in this study, it should be noted that the time constraint can be adjusted to appropriately target skeletal injuries based on correlation with physical test data. However, regardless of selected time constraint, it was observed that female HBMs showed significantly higher injuries than M50, as seen in Fig. 15 (b).

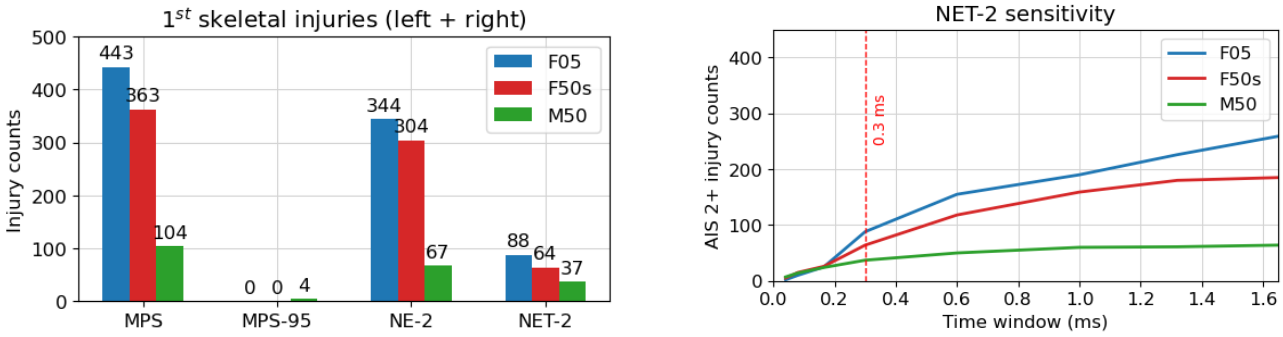

(a) (b)

Fig. 15. (a) Bone fracture criteria and (b) NET-2 sensitivity to selected time window.

NET-2 skeletal injuries, stratified by left and right foot, are shown in Fig. 16 (a) and the right foot, once again, showed higher risk of skeletal injuries compared to left foot, except for the F05 HBM. The combined (left + right) female vs male odds ratio for skeletal injuries were 2.6 for F05 and 1.8 for F50s. Figure 16 (b) shows the distribution of all skeletal injuries by sex, and it was observed that female HBMs showed higher risk of Malleolar Tibia fractures, whereas the M50 HBM showed higher risk for Talus fractures.

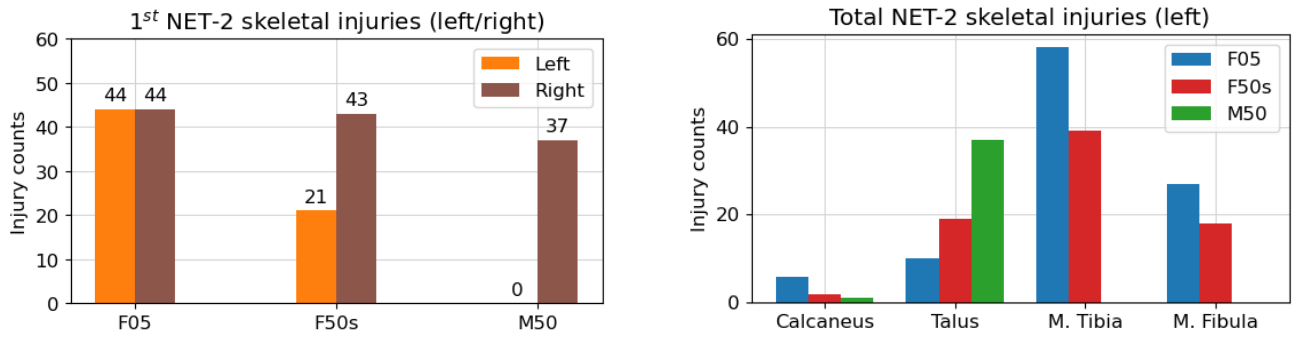

(a) (b)

Fig. 16. (a) AIS2+ NET-2 skeletal injuries and (b) distribution of total skeletal injuries.

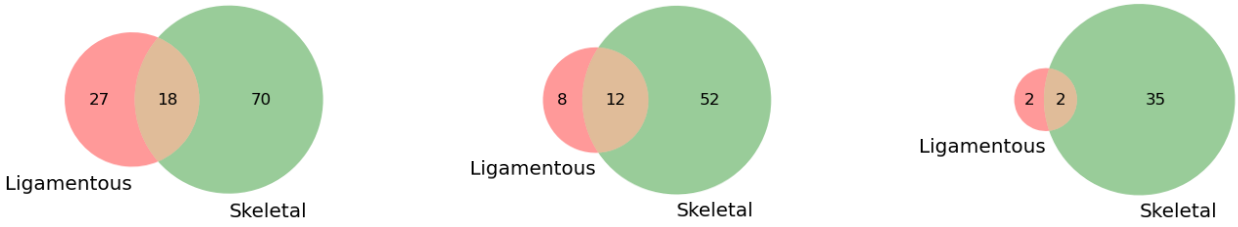

(a) (b) (c)

Fig. 17. AIS2+ injuries for (a) F05 (b) F50s and (c) M50.

Figure 17 aggregates all injuries (left + right) and compares the number of exposures with either ligamentous only, skeletal only, or both ligamentous and skeletal injuries. It was observed that NET-2 skeletal injuries were dominant in all HBMs, and that ligamentous injuries in several cases were accompanied by skeletal injuries.

To evaluate and compare the influence of DOE design variables on resulting skeletal injuries, a Radial Basis Function Network (RBFN) metamodel was generated within LS-OPT. The continuous response, or the output variable in this case, was the time-history max MPS out of four bones (per foot). Metamodel accuracies, computed in the form of coefficient of determination (R^2) between the observed outcome and the predicted value of max MPS, and the global sensitivities (variance-based) for each design variable, computed using Sobol's method [24], are listed in TABLE IV. The global sensitivity index represents the fraction of influence that specific design variable has on the output variable i.e., higher the sensitivity index, higher the influence.

TABLE IV
METAMODEL ACCURACIES AND GLOBAL SENSITIVITY INDICES (%)

Left foot			Design variables	Right foot		
F05	F50s	M50		F05	F50s	M50
0.96	**0.98**	**0.87**	***Metamodel accuracies (R^2)***	**0.78**	**0.88**	**0.79**
77.9	72.4	56.5	*Delta-V*	94.0	92.2	79.3
15.4	24.1	37.5	*PDOF*	3.4	2.9	6.2
1.2	1.7	3.2	*SLL*	0.5	2.3	2.6
3.4	0.8	1.6	*SP*	1.1	0.7	3.4
0.6	0.3	0.3	*BPRS*	0.2	0.2	4.9
1.4	0.8	0.9	*NKD*	0.7	1.7	3.7

It was observed that max MPS in the right foot was most influenced by Delta-V, whereas in the left foot, it was influenced by both Deltav-V and PDOF. By isolating paired runs for all HBMs at 20 mph (42 exposures, Fig. 13 (a)) and re-evaluating the global sensitivity indices for the remaining variables (TABLE V) it was observed that the relative contributions of seatbelt pretensioner force (SP), seatbelt load limiter force (SLL) and normalised knee to dash distance (NKD) grow significantly, indicating that optimising restraint parameters could potentially help mitigate some ankle injuries.

TABLE V
GLOBAL SENSITIVITY INDICES (%) @ 20 MPH

Left foot			Design variables	Right foot		
F05	F50s	M50		F05	F50s	M50
21.9	70.7	67.3	*PDOF*	4.1	31.4	42
3.9	1.3	3.7	*SLL*	35.6	21.3	22
46.3	25.5	12.7	*SP*	43.5	9.6	17.8
7.4	0.3	3.6	*BPRS*	2.6	0.4	5.7
20.5	2.3	12.7	*NKD*	14.3	37.3	12.4

Note: Since normalised knee to dash distance (NKD) and BPSA had a strong correlation post sampling, the relative increase in NKD's influence on max MPS may be coming from the variations in BPSA as well.

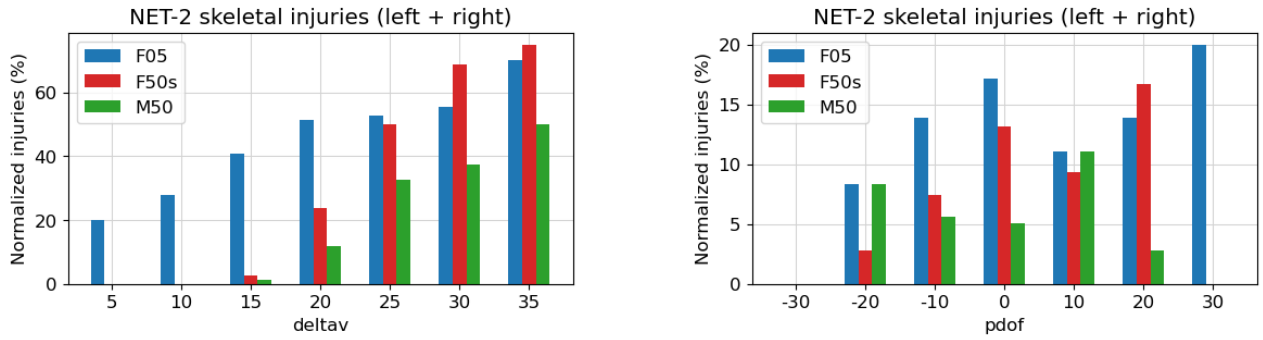

(a) (b)

Fig. 18. NET-2 skeletal injuries normalised by number of simulation points for (a) Delta-V and (b) PDOF.

The distribution of combined skeletal injuries, normalised by respective sampling frequencies of Delta-V and PDOF, is shown in Fig. 18 (a) and Fig. 18 (b), respectively. The influence of Delta-V on skeletal injuries was once

again confirmed here with a strong positive correlation for all three HBMs. It was also observed that the risk of skeletal injuries to female HBMs at 25 mph was similar to the risk to M50 at 35 mph. Comparing averaged injuries in near-side (-30° to -10°), far-side (10° to 30°) and full-frontal (0°) impacts, normalised by number of individual PDOF runs, it was observed that female HBMs showed highest risk in full-frontal impacts (17% for F05 and 13% F50s) and almost twice the risk in far-side than in near-side impacts (15%/7% for F05 and 8%/3% for F50s), whereas M50 showed relatively lower risk across all PDOFs (5% in full-frontal and 4% in near/far-side impacts).

IV. DISCUSSION

To better understand crash induced ankle injuries, and their distribution among females and males, this study utilised three different HBMs, two of which were validated GHBMC models (F05 and M50). A scaled version of the 5th female (F50s) was also introduced to assess injury risks based on the anthropometry of a mid-sized female. These modular models, with simplified pelvis and upper body and detailed lower extremities, allowed for simulating a wide range of frontal impact scenarios using the DOE method. Compared to the detailed GHBMC models, these FE models lowered the simulation runtime by a factor of three, while preserving model fidelity in the foot and ankle region. All HBMs were positioned in the simplified occupant compartment model using representative measurements from physical NHTSA tests. Distinct boundary conditions for the left vs right foot were utilised, by positioning the right foot on the brake pedal and the left foot in the toepan region. This not only doubled the size of the ankle injury dataset, but also provided for additional insights into resulting injury distributions. GHBMC HBMs came pre-programmed with ligament and skeletal (cortical bone) injury parameters that were used to access and investigate the risk of AIS2+ injuries, based on 1st recorded injury per foot. However, due to lack of sufficient ligament failure test data, the following discussion is primarily focused on skeletal injuries. Two additional bone fracture criteria (NE-2 and NET-2) were introduced, which allowed us to identify bone fractures consistently across all HBMs and bones. LS-OPT DOE was then utilised to design and execute paired simulations for all three HBMs, and it included field representation of vehicle crash parameters such as Delta-V and PDOF. This enabled focusing the investigation on real-world CIIs and compare resulting injury distributions to comparable field data analysis, such as in [6]. The DOE also included seatbelt restraint parameters, brake pedal stop angle and rotational stiffness, and relative position of the HBM with respect to knee bolster as design variables. This enabled simulating a wide range of mid-sized sedans and investigating the influence of these design variables on resulting ankle injuries.

The results demonstrate that MPS and MPS-95 may not be suitable for identifying bone fractures due to their inability to filter out spurious single element strains. Results also show that NET-2 eliminated spurious single element strains using NE-2, and further ensures that a fracture is registered only if constituent elements of the local cluster exceed failure strain within 0.3 ms of each other. Another feature of the NET-2 criterion is its ability to adjust the time constraint based on correlation with physical test data.

Results also show that under similar crash conditions (field representative), female HBMs show significantly higher ankle injuries than the male HBM (Fig. 16 (a)). It was observed that the un-weighted odds ratio for female vs male HBM injuries are 2.6 for F05 and 1.8 for F50s. This observation was in agreement with [6][27] in which the authors concluded that female drivers are at a greater risk for foot and ankle injuries, 1.86 times more likely as per [27] for 1994-2007 NASS-CDS cases, and 3.8 times more likely as per [6] for 1998-2015 NASS-CDS cases.

Note: The data utilised by [6][27] were weighted according to NASS-CDS recommendations for analysed populations. Reference [27] also concluded that shorter occupants sustained more foot and ankle injuries than their taller counterparts, which was also observed in this study for relative injuries among F05, F50s and M50 HBMs. This difference in ankle injuries could be attributed to the relative seating positions of shorter vs taller HBMs, and the resulting foot interactions with the brake pedal and the toepan.

It was also observed that the right foot, when positioned on the brake pedal, showed relatively higher injuries than left foot, except for the F05 HBM (Fig. 16 (a)). This observation agreed with [28], in which the authors show that drivers are more likely to sustain foot and ankle injuries, than passengers, almost exclusively due to the higher frequency of right foot injuries. They also show that this increase in right foot injuries is primarily due to the combined dorsiflexion and eversion of the foot, when engaged with the brake pedal. Results also show that Malleolar Tibia (for female HBMs) and Talus (for male HBM) are among the most common skeletal injuries (Fig. 16 (b)), which was also consistent with the findings by [29].

Variance-based global sensitivity analysis of the design variables also show that foot and ankle injuries are

most influenced by Delta-V (TABLE IV), and the strong positive correlation between ankle injuries and Delta-V (Fig. 18 (a)) is also in agreement with AIS2+ foot and ankle injury risk based on Delta-V by [27].

V. CONCLUSION

Given the scope of simulated paired runs for the analysed HBMs, with field representative sampling for vehicle crash parameters such as Delta-V and PDOF, the following conclusions may be drawn:

1. GHBMC modular models enable lowering simulation runtime while preserving model fidelity in the lower extremity BRM, enabling the simulation of a wide range of frontal impact cases for a comprehensive foot and ankle injury assessment.
2. Simulating field distribution of critical crash parameters such as Delta-V and PDOF allowed evaluating injury risks that are representative of real-world CIIs, and accordingly provided valuable insights in investigating field critical injury mechanisms.
3. A new bone fracture criterion (NET-2) provided a consistent approach to identifying skeletal injuries across all HBMs, with the ability to filter out spurious single element strains, as well as the elements with respective peak strains temporally separated.
4. Female HBMs (F05 and F50s) show significantly higher risk for NET-2 skeletal injuries than the male HBM (M50), with an un-weighted odds ratio of 2.6 for F05 and 1.8 for F50s.
5. Malleolar Tibia and Talus show higher risk of injury for female and male HBMs, respectively.
6. Right foot (positioned on the brake pedal) consistently showed higher injuries than left foot (positioned in the toepan), with exception of F05 for which left and right foot have equal injury counts.
7. Recorded response for the maximum MPS (out of four bones, stratified by foot) was observed to be most influenced by Delta-V and PDOF, followed by the restraint parameters such as SP and SLL for the 20 mph dataset.
8. Finally, this study also demonstrates that simulation-based CII investigations, using HBMs, may provide valuable insights into injury causing mechanisms, and may be a useful tool in building injury risk functions.

VI. DISCLAIMER

This report is published in the interest of advancing motor vehicle safety research. The United States Government assumes no liability for its contents or use thereof. If trade or manufacturers' names are mentioned, it is only because they are considered essential to the object of the publication and should not be construed as an endorsement. The United States Government does not endorse products or manufacturers.

VII. REFERENCES

[1] Klinich, K. D., Bowman, P., Flannagan, C. A. & Rupp, J. D. Injury Patterns in Motor-Vehicle Crashes in the United States: 1998 – 2014, Washington, DC: National Highway Traffic Safety Administration. 2016.

[2] Qin, X., Wang, K. & Cutler, C. E. Analysis of Crash Severity Based on Vehicle Damage and Occupant Injuries. *Journal of the Transportation Research Board*, 2013, 2386(1), pp. 95-102.

[3] Frampton, R. et al. Effectiveness of airbag restraints in frontal crashes: What European field studies tell us. Montpellier, France, *Proceedings of the 2000 International IRCOBI conference on the biomechanics of impact*. 2000.

[4] MacLennan, P. A. et al. Risk of injury for occupants of motor vehicle collisions from unbelted occupants. *Injury prevention: Journal of the International Society for Child and Adolescent Injury Prevention*, 2004, 10(6), pp. 363-367.

[5] Kahane, C. J. Effectiveness of Pretensioners and Load Limiters for Enhancing Fatality Reduction by Seat Belts, Washington, DC: National Highway Traffic Safety Administration. 2013.

[6] Forman, J. et al. Automobile injury trends in the contemporary fleet: Belted occupants in frontal collisions. *Traffic injury prevention*, 2019, 20(6), pp. 607-612.

[7] Read, K. M. et al. Life-altering outcomes after lower extremity injury sustained in motor vehicle crashes. *The Journal of trauma*, 2004, 57(4), pp. 815-823.

[8] Bose, D., Segui-Gomez, M. & Crandall, J. R. Vulnerability of female drivers involved in motor vehicle crashes: an analysis of US population at risk. *American journal of public health*, 2011, 101(12), pp. 2368-2373.

[9] Dischinger, P. C., Kerns, T. J. & Kufera, J. A. Lower extremity fractures in motor vehicle collisions: the role of driver gender and height. *Accident Analysis & Prevention*, 1995, 27(4), pp. 601-606.

[10] Crandall, J. et al. Foot and ankle injury: the roles of driver anthropometry, footwear, and pedal controls. Vancouver, BC, Canada, *Proceedings of the 40th annual conference of the association for the advancement of automotive medicine*. 1996.

[11] Ye, X. et al. Analysis of crash parameters and driver characteristics associated with lower limb injury. *Accident Analysis & Prevention*, 2015, 83, pp. 37-46

[12] Singh, H., Ganesan, V., Davies, J., Paramasuwom, M., & Gradischnig, L. Vehicle Interior and Restraints Modeling Development of Full Vehicle Finite Element Model Including Vehicle Interior and Occupant Restraints Systems for Occupant Safety Analysis Using THOR Dummies, Washington, DC: National Highway Traffic Safety Administration. 2018.

[13] Fitch, G. M, Blanco, M., Morgan, J. F., Rice, J. C., Wharton, A. E., Wierwille, W. W., & Hanowski, R. J. Human Performance Evaluation of Light Vehicle Brake Assist Systems, Washington, DC: National Highway Traffic Safety Administration. 2010.

[14] Hansen, V. & Dutton, E. Report for Frontal Oblique Offset Program Testing of a 2015 Chevrolet Malibu four door sedan, Washington, DC: National Highway Traffic Safety Administration. 2016.

[15] Global Human Body Models Consortium. User Manual: F05 Detailed Occupant Version 5.1 for LS-DYNA. Clemmons, NC: Elemance LLC. 2020.

[16] Global Human Body Models Consortium. User Manual: M50 Detailed Occupant Version 5.1.1 for LS-DYNA. Clemmons, NC: Elemance LLC. 2020.

[17] McDowell, M. A., Fryar, C. D. & Ogden, C. L. Anthropometric reference data for children and adults: United States, 1988-1994. *Vital and health statistics*, 2009, 11, pp. 1-68.

[18] Schneider, L. W., Robbins, D. H., Pflug, M. A. & Snyder, R. G. Development of anthropometrically based design specifications for an advanced adult anthropomorphic dummy family, volume 1, Washington, DC: National Highway Traffic Safety Administration. 1983.

[19] Lewandowski, J. Final Report of FMVSS 208 Compliance Testing of a 2013 Honda Accord, Washington, DC: National Highway Traffic Safety Administration. 2013.

[20] Chiu, K. A. & Richardson, F. Final Report of New Car Assessment Program Testing of a 2013 Honda Accord EX-L 4-Door Sedan, Washington, DC: National Highway Traffic Safety Administration. 2012.

[21] Funk, J., Hall, G., Crandall, J. & Pilkey, W. Linear and quasi-linear viscoelastic characterization of ankle ligaments. *Journal of biomechanical engineering*, 2000, 122(1), pp. 15-22.

[22] Funk, J., Tourret, L., George, S. & Crandall, J. The Role of Axial Loading in Malleolar Fractures. *SAE transactions*, 2000, 109, pp. 212-223.

[23] Nie, B. et al. Determination of the in situ mechanical behavior of ankle ligaments. *Journal of the Mechanical Behavior of Biomedical Materials*, 2017, 65, pp. 502-512.

[24] Livermore Software Technology Corporation. LS-OPT User's Manual: A design optimization and probabilistic analysis tool for the engineering analyst. Livermore: LSTC. 2020.

[25] Shannon, D., Murphy, F., Mullins, M. & Rizzi, L. Exploring the role of delta-V in influencing occupant injury severities - A mediation analysis approach to motor vehicle collisions. *Accident analysis and prevention*, 2020, 142(105577).

[26] Takhounts, E. G., Hasija, V. & Craig, M. J. BrIC and Field Brain Injury Risk. Eindhoven, Netherlands, *26th International Technical Conference on the Enhanced Safety of Vehicles (ESV): Technology: Enabling a Safer Tomorrow*. 2019.

[27] Rudd, R. W. Updated analysis of lower extremity injury risk in frontal crashes in the United States. *Proceedings Of the 21st International Technical Conference on the enhanced safety of vehicles (ESV)*, Stuttgart, Germany. 2009.

[28] Assal, M., Huber, P., Tencer, A. F., Rohr, E., Mock, C. & Kaufman, R. Are drivers more likely to injure their right or left foot in a frontal car crash: a crash and biomechanical investigation. *Annual Proceedings: Association for the Advancement of Automotive Medicine*, 2002, 46, pp. 273-288.

[29] Funk, J. R., Rudd, R. W., King, R. J., Srinivasan, S., Bailey, A. M. & Crandall, J. Injuries caused by brake pedal loading of the midfoot. *Biomedical Sciences Instrumentation*, 2012, 48, pp. 134-140.